

Indirect Amperometric Detection of Non-Electroactive Species: Towards an Electrochemical Bioassay of Mineral Weathering?

Alain Walcarius^{1,*} and Christian Mustin²

¹ *Laboratoire de Chimie Physique et Microbiologie pour l'Environnement (LCPME), UMR 7564, CNRS – Nancy-University, F-54602 Villers-les-Nancy, France;*

² *Laboratoire des Interactions Microorganismes-Minéraux-Matière Organique dans les Sols (LIMOS), UMR 7137, CNRS – Nancy-University, Faculté des Sciences, BP 70239, F-54602 Vandoeuvre-les-Nancy, Cedex, France.*

Abstract: Ion exchange polymers doped with a suitable electroactive mediator (*i.e.*, Cu²⁺ or Fe(CN)₆³⁻) have been used to modify carbon paste electrodes that have been further applied to the indirect amperometric detection of non-redox cations or anions in flow injection analysis. The detection mechanism involves ion exchange between the non-redox ionic analyte and the electroactive mediator, in the polymer particles located at the electrode surface, followed by the electrochemical transformation of the mediator species leached out of the polymer at the electrode/solution interface. Operating in the absence of added supporting electrolyte led to peak currents made of a major faradic component that is added to a capacitive contribution due to the conductivity jump occurring upon the analyte passing the electrode surface. The method can be applied to the detection of non-electroactive mineral cations and anions, as well as poorly-dissociated organic acids, which are usually involved in mineral weathering. After having characterized and discussed the main parameters affecting the sensitivity of the detection (with respect to analyte charge, size and degree of dissociation), the electrochemical device was evaluated as a possible test to monitor mineral weathering in a simple case (zeolite dissolution in acidic medium) and in a more sophisticated one (biomediated olivine dissolution by fungi).

Keywords: Carbon paste electrode; Indirect amperometric detection; Flow injection analysis; Ion exchangers; Organic acids; Mediators; Biomineralization; Water samples.

*) Author to whom correspondence should be addressed. E-mail: alain.walcarius@lcpme.cnrs-nancy.fr

Introduction

Even if ion-selective electrodes and potentiometry are still today effective for non-redox ions [1-5], their logarithmic response make them less sensitive than other techniques, as amperometry, giving rise to linear response to the analyte concentration. This is one reason why the past two decades have seen the development of novel methods directed to the amperometric detection of electroinactive ions [6-38], with possible applications in combination to ion chromatography or capillary electrophoresis [8-10,12,13,18,19,23,25-27, 30,32,33,37,38]. As detailed hereafter, they include the electrochemical doping/de-doping of conducting polymers, the electrochemically-assisted ion transfer at liquid/liquid interfaces, or the resort to zeolite modified electrodes doped with suitable redox probes.

The first approach involves the electrochemical transformation of organic polymers (polypyrrole, polypyrrole-alkylsulphonate, polyaniline, poly-o-phenylenediamine, *etc.*), which can only occur if charge-compensating ions pass the electrode to enable the incorporation of such ionic species to counterbalance the electric charge generated by the electron transfer reaction. Under potential control, such electrodes generate indeed current values proportional to the concentration of non-redox counter ions [6,7,10,12-15,18-20,32,33] but they can suffer from poor long-term stability because the conducting polymers are likely to exhibit structural changes during the doping-dedoping process, resulting in selectivity changes [39]. Other electroactive films such as inorganic polyoxometallates [8,9,17,31] and mixed metal oxides [21] can be also used for indirect amperometric detection.

The second basic approach exploits the electrochemically-assisted ion transfer at liquid/liquid interfaces [22-25,34], generating an amperometric signal due to the ion transfer across the interface, measured upon the application of a selected potential difference, which is related to the concentration of the ionic components in the aqueous phase [22,26]. For example, polarized organic gel/water microinterfaces have been described as selective transducers for the amperometric detection of non-redox ions in ion chromatography [23].

The third approach is based on the particular electrochemical behavior of zeolite modified electrodes (ZMEs) that exploit the combination of ion exchange and size selectivity properties of zeolites [40,41]. When small electroactive mediators (size less than that of the zeolite pore apertures: Cu^{2+} for example) are exchanged within a ZME, the mechanism responsible for charge transfer is their exchange for the electrolyte cation followed by their electrochemical transformation outside the zeolite framework [42]. Therefore, the currents measured at such electrode can be related to the concentrations of the non-electroactive

electrolyte cations when they are small enough to penetrate the zeolite framework and to expel the mediator species out of the molecular sieve. This principle can be applied for the indirect amperometric detection of alkali metal, alkaline earth, and ammonium ions, either in bulk solutions [11] or by flow-injection analysis [16,28,29]. It was then demonstrated that such detection at ZMEs can be performed in the absence of supporting electrolyte, leading to its possible application as a detector in suppressed ion chromatography [30], and opening the door to the use of other electrode modifiers (*i.e.*, without size-selectivity properties), as cation or anion exchange resins doped with a suitable charge transfer mediator [43]. In such detection pathway, the ionic species pass the electrode surface in a transient way, acting as both the electrolyte and the real analyte (the current response has two origins: a capacitive one and an (indirect) faradic one) [30,43]. So far, this detection scheme using ZMEs or ion-exchanger modified electrodes was restricted to cations such as Li^+ , Na^+ , K^+ , Cs^+ , Rb^+ , NH_4^+ , Ca^{2+} , and Mg^{2+} , or anions like F^- , Cl^- , NO_2^- , NO_3^- , SO_4^{2-} , and PO_4^{3-} [16,27-30,36,43].

In the present work, we have evaluated the potentiality of this method to monitor mineral weathering processes. These processes, and especially biological mineral weathering, play a major role in the release and cycling of essential nutrients (Fe, Mg, Ca, *etc.*) required for living organisms and contribute, then, to soil fertility [44-50]. Indeed, a large amount of soil microorganisms (*i.e.*, bacteria and fungi) act directly or indirectly on several dissolution processes affecting aluminosilicates integrity and oligo-element availability from mineral surface to entire ecosystem [45,46]. Therefore, the interest in the assessment of mineral weathering processes raise new technical issues, such as the development of rapid assays or sensors for monitoring microbial activities in natural environment [47,50]. The indirect amperometric response described above is thus likely to basically offer a way, yet qualitative, to monitor changes in the ionic composition of these (yet complex) media and to detect chemical or biological mobilization of elements (*e.g.*, Mg) from mineral. This is the potentiality of designing an electrochemical bioassay of mineral weathering, based on electrodes modified with redox-doped ion exchangers, we would like to investigate here. The experiments were based on carbon paste electrodes modified with either a polycationic or a polyanionic polymer containing a suitable charge transfer mediator ($\text{Fe}(\text{CN})_6^{3-}$ or Cu^{2+}), operating in an indirect amperometric mode. As the mechanisms responsible for mineral weathering by microorganisms usually involve both the production of organic acids (by the bacteria) [45-47] and leaching of mineral ions, it was necessary to first characterize the electrode response in such media. Then, after having examined a model reaction of mineral weathering (zeolite dissolution in acidic medium), a first real-case analysis (biomediated olivine dissolution by fungi) has been performed.

Experimental

Chemicals and Reagents

All chemicals used for the preparation of stock solutions were of analytical reagent grade and purchased from *Sigma-Aldrich* or *Merck*. All solutions were prepared with high purity water ($18 \text{ M}\Omega \text{ cm}^{-1}$) from a Millipore Milli-Q water purification system.

The ion exchange polymers used here are the cationic resin Amberlite IR-120 and the anionic resin Amberlite IRA-910, purchased from Sigma-Aldrich. They are made from a styrene-divinylbenzene matrix containing covalently-attached sulfonate (IR-120) or quaternary ammonium (IRA-910) groups, both of them exhibiting an average particle size of 650-700 μm . They were conditioned in pure water during 48 hours before use.

Electrode Preparation

Loading Ion-exchange Resins with Redox Probes. IR-120 was loaded with Cu^{2+} species by suspending typically 2 g of the resin into 250 ml of a 0.02 M $\text{Cu}(\text{NO}_3)_2$ solution, and allowing it to react during 48 hours. The suspension was then filtered and the solid particles were suspended again in a fresh 0.02 M $\text{Cu}(\text{NO}_3)_2$ solution for 48 hours. After filtration and washing with copious amounts of pure water, the solid was allowed to dry at room temperature. The same protocol was applied to load the IRA-910 resin with $\text{Fe}(\text{CN})_6^{3-}$ species, by using a $\text{K}_3\text{Fe}(\text{CN})_6$ solution instead of $\text{Cu}(\text{NO}_3)_2$. The experimental capacities were 0.13 and 0.16 mmol g^{-1} , respectively for Cu^{2+} -IR-120 and $\text{Fe}(\text{CN})_6^{3-}$ -IRA-910, as determined by atomic absorption spectrometry for copper (Philips, model PU9200X) and by cyclic voltammetry for hexacyanoferrate. When required, the polymer particles were ground for selected periods of time in an automated mortar (Pulverisette II, Fritsch), the resulting material being characterized by using the Horiba laser scattering particle size distribution analyzer LA920; the measuring principle being based on Mie scattering theory. The apparatus was equipped with two light sources: a He-Ne laser (632.8 nm) and a W halogen lamp.

Construction of Modified Carbon Paste Electrodes. Modified carbon paste electrodes were prepared in a similar way as that previously described for powdered ion exchange modifiers [28,30,42,43]. High purity graphite powder (325 mesh, Johnson Matthey) was first mixed with the polymer particles in 6:1 mass ratio. 300 mg of mineral oil (Nujol, Aldrich) was then added to 700 mg of this mixture and the resulting material was homogenized to obtain a

uniformly wetted paste. The paste was packed into the end of a PTFE body equipped with a screwing stainless steel piston, which was designed to be adapted on the home-made flow-through cell (see below). When necessary, regeneration of the electrode surface was performed by mechanical polishing on a weighing paper.

Instrumentation and Analytical Procedures

The full experimental assembly used for the indirect amperometric detection of non-electroactive species is depicted in Fig. 1.

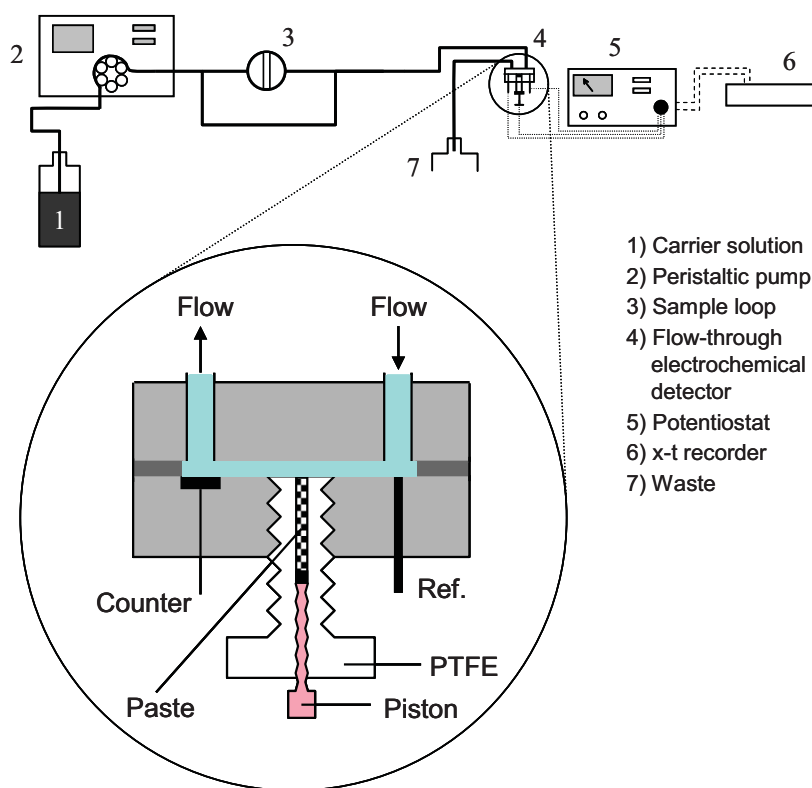


Fig. 1: Schematic representation of the experimental device for the flow injection analysis of non-redox species at carbon paste electrode modified with resins exchanged with redox probes.

The home-made microcell (schematic view enlarged on Fig. 1) used for the amperometric detection was a thin-layer cavity, composed of two 6.0 cm × 4.0 cm × 1.5 cm (l × w × h) polymeric blocks (epoxy and Altuglas), which were separated by a *Teflon*[®] spacer.

The lower epoxy block was machined to mold a Pt-plate and a Ag-wire in defined positions at the inner surface of the block. Platinum and silver acted as the counter and quasi-reference electrode, respectively. The PTFE working electrode body was inserted between these two electrodes by screwing it through the epoxy block, leaving it free to be easily removed for regeneration purpose. Two holes were drilled in the upper *Altuglas*[®] block and were equipped with *Omnigrip*[®] fittings for connection to the sample loop (with an inner volume of 100 μl) via 1/16-inch Teflon tubing (with 1.6 mm in diameter).

Reference and counter electrodes were arranged so that they were opposite to the inlet and outlet holes when the two blocks were placed together and bolted down with Nylon machine screws at each corner. The window of the Teflon spacer (with thickness of 500 μm) extended from the inlet to the outlet holes, resulting in a thin channel of 70 μl volume. Flow rate was typically 5.0 ml min^{-1} , using pure water as the mobile phase (*i.e.*, carrying flow). The measurements performed with the amperometric sensor were conducted with the aid of a potentiostat model 362A (EG&G Princeton Applied Research).

Mineral Weathering Experiments

Two kinds of experiment were performed. The first one was the chemical weathering of zeolites A and Y (30 mg L^{-1}) in citric acid (10^{-4} M). Zeolite Y ($\text{Na}_{56}\text{Al}_{56}\text{Si}_{136}\text{O}_{384}\cdot 250 \text{H}_2\text{O}$) was the Linde Molecular Sieve Cat. Base L-Y54 powder obtained from UOP, Molecular Sieve Division, and zeolite A ($\text{Na}_{12}\text{Al}_{12}\text{Si}_{12}\text{O}_{48}\cdot 27 \text{H}_2\text{O}$) was purchased from Strem Chemicals. Both zeolite samples were available in their sodium forms (cation exchange capacities: 5.6 meq g^{-1} for NaA and 3.4 meq g^{-1} for NaY).

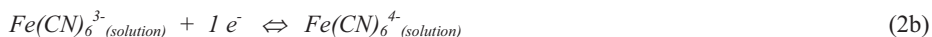
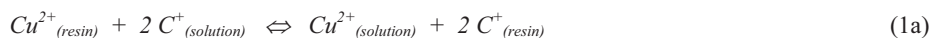
The second one was the bacterial weathering of a magnesium rich olivine (forsterite like: $(\text{Fe}_y\text{Mg}_{2-y})\text{SiO}_4$, $y < 0.5$). Experiments were performed, in duplicate (samples A and B), by mixing 0.5 g ground specimens (250-500 μm) of olivine in 100 ml of mineral media supplemented in glucose [47] inoculated with *Aspergillus niger* (fungus strain DSM 821). Reactors were incubated at 24°C in the dark during four weeks.

Prior to electrochemical and chemical analysis, leachates were collected and filtered at 0.22 μm . An abiotic control experiment (incubation without fungi) was used as baseline for electrochemical detection (Mg^{2+} calibration was made in this medium).

Results and Discussion

Fundamentals and Factors Affecting the Amperometric Response

The amperometric detection principle is based on the particular electron transfer mechanism characterizing the behavior of either Cu^{2+} -IR-120 or $\text{Fe}(\text{CN})_6^{3-}$ -IRA-910 modified carbon paste electrodes (MCPEs). As the ion exchange polymers (Cu^{2+} -IR-120 and $\text{Fe}(\text{CN})_6^{3-}$ -IRA-910) are not electronically conductive, the only way for the mediator to undergo an electron transfer is its leaching out of the polymer, in close proximity to the electronically conductive electrode surface [43]. This is achieved by ion exchange of the mediator for the electrolyte cation C^+ (for Cu^{2+}) or anion A^- (for $\text{Fe}(\text{CN})_6^{3-}$), which can be followed by the charge transfer reaction of the leached mediator species (Eqs. 1&2).



As a result, the electrochemical response of the redox probes (initially incorporated into the ion exchange resins) can be basically related to the concentration of ions (C^+ or A^-) in solution because they contribute to liberate the probes at the electrode/solution interface by ion exchange (Eqs. 1a & 2a), enabling therefore their subsequent amperometric detection (Eqs. 1b & 2b). Note that when working in the absence of added supporting electrolyte, which is the case here, the overall amperometric response is the sum of a faradic contribution (*i.e.*, that corresponding to the above reactions 1b & 2b) and a capacitive one due to the presence of charged species at the electrode/solution interface).

This detection pathway has been applied here in flow injection analysis (FIA) using an electrolyte-free aqueous solution carrier in potentiostatic conditions. The applied potential was found to have significant influence on both the current background and the amperometric peak heights obtained upon injection of cationic or anionic analytes (*e.g.*, Na^+ detected at Cu^{2+} -IR-120-MCPE, see Fig. 2A). As expected, the response to the injected ionic analyte was found to increase when shifting potentials towards more cathodic values but this also contributed to increase the unwanted background currents.

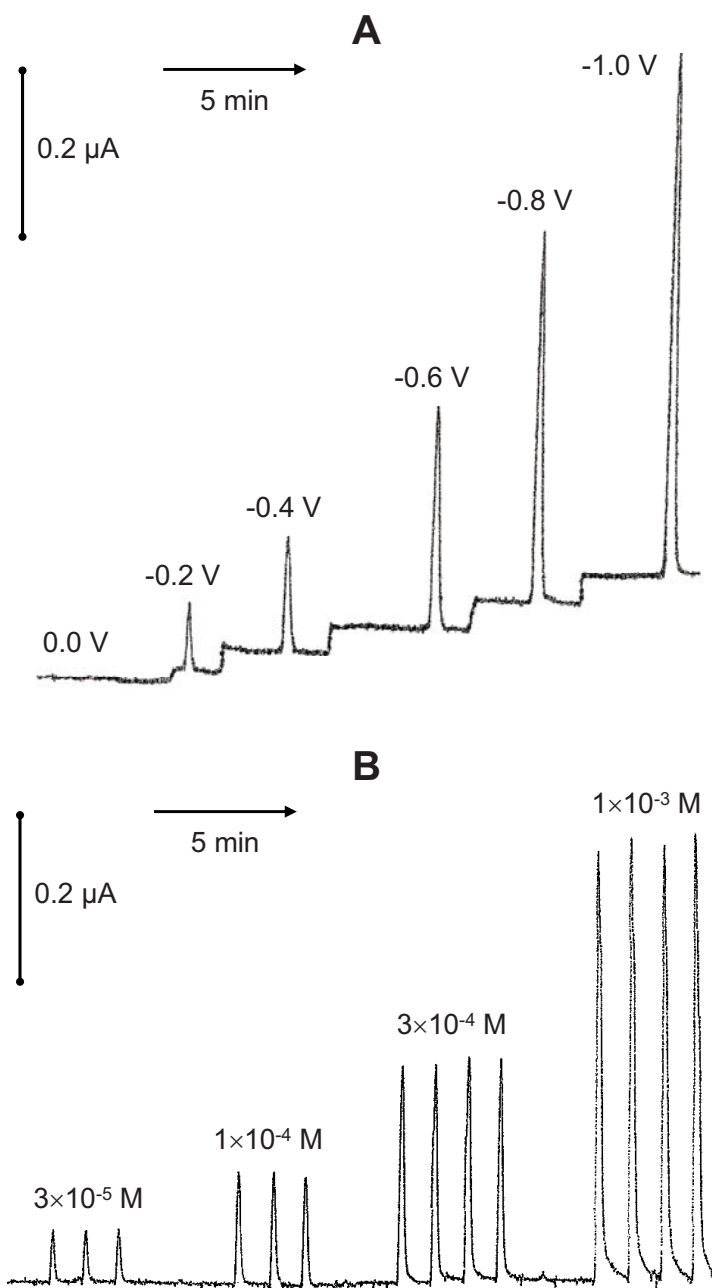


Fig. 2: Flow injection amperometric responses of Cu^{2+} -IR-120 polymer (10%) modified carbon paste electrodes to 100 μl injections of NaNO_3 (actually detected as Na^+): (A) effect of the applied potential on the detection of $1.0 \times 10^{-4} \text{ M Na}^+$; (B) variation of the amperometric response upon successive injections of the analyte at increasing concentrations ($3.0 \times 10^{-5} \text{ M}$, $1.0 \times 10^{-4} \text{ M}$, $3.0 \times 10^{-4} \text{ M}$, $1.0 \times 10^{-3} \text{ M}$). Carrier solution: pure water. Flow rate: 5.0 ml min^{-1} . (B) applied potential: -0.4 V .

The best compromise ensuring the optimal signal-to-noise ratio was -0.4 V (actually for both Cu^{2+} -IR-120-MCPE and $\text{Fe}(\text{CN})_6^{3-}$ -IRA-910-MCPE). Increase of concentrations in the electrolyte had resulted in larger amounts of leached species and, therefore, in higher amperometric responses (see *e.g.* Fig. 2B). Repetitive analyses of the same sample also reveal quite good reproducibility of measurements. Actually, standard deviations less than 3 % were typically observed and the electrode response remained stable for at least 50 successive measurements (no detectable signal decrease in such conditions).

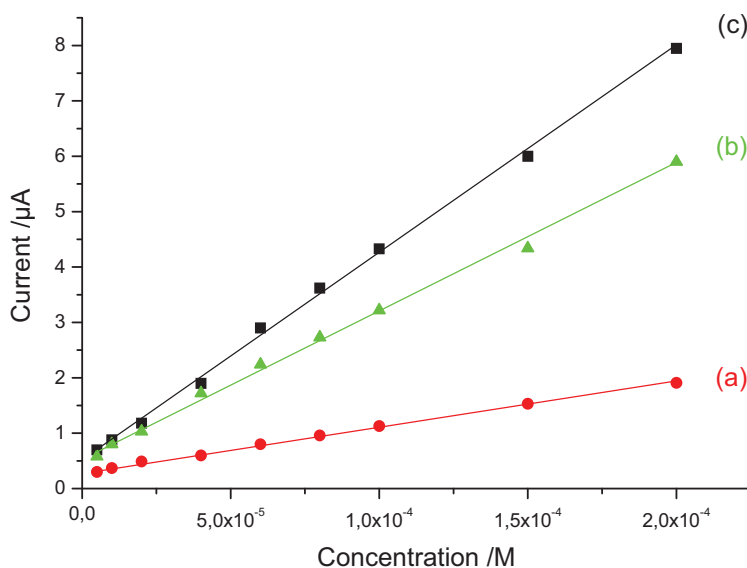


Fig. 3: Variation of the amperometric response of (a) unmodified CPE, (b) Cu^{2+} -IR-120-MCPE, and (c) $\text{Fe}(\text{CN})_6^{3-}$ -IRA-910-MCPE, to NaNO_3 concentrations in the 1.0×10^{-5} M to 2.0×10^{-4} M concentration range. Other conditions as those in Fig. 2.

The sensitivity of the amperometric response was dependent of the used electrode, giving rise to slightly larger values for $\text{Fe}(\text{CN})_6^{3-}$ -IRA-910-MCPE in comparison to Cu^{2+} -IR-120-MCPE, as illustrated for the analysis of NaNO_3 in the 10^{-5} M to 2×10^{-3} M concentration range (Fig. 3). Peak currents were directly proportional to the analyte concentration in that range. As also shown, the use of an unmodified carbon paste electrode also led to the possible detection of NaNO_3 by amperometry. Of course, this response cannot be due to any faradic current but are ascribed to capacitive currents originating from the change in the conductivity of the carrier solution upon the injection of the sodium nitrate sample.

Comparison between currents observed at unmodified CPE and those recorded using the electrodes modified with $\text{Fe}(\text{CN})_6^{3-}$ -IRA-910 or Cu^{2+} -IR-120 indicates that the main part of the indirect amperometric response is due to the faradic contribution originating from the above scheme involving the exchange and subsequent detection of redox probes from the polymers (see Eqs. 1&2).

Influence of the Nature of the Analytes

Two series of ionic analytes have been first investigated: in the first one, the anion was kept the same (NO_3^-) and cations varied, while the second one was the opposite (variation of anions with keeping the same Na^+ cation). As shown in Table I, the electrode response was significantly affected by the nature of the ion, and especially by its charge. For instance, in the cationic series, the response of Cu^{2+} -IR-120-MCPE was found to increase regularly when passing from monovalent to divalent and to trivalent cations. The same trend was observed using $\text{Fe}(\text{CN})_6^{3-}$ -IRA-910-MCPE, which is explained by increasing concentrations of the charge-compensating anions (NO_3^-).

Table I: FIA peak currents (μA) sampled for the analysis of various analytes (10^{-4} M) using either Cu^{2+} -IR-120-MCPE or $\text{Fe}(\text{CN})_6^{3-}$ -IRA-910-MCPE at an applied potential of -0.4 V.

Cationic series			Anionic series		
Injected solution (0.1 mM)	Cu^{2+} -IR- 120-MCPE	$\text{Fe}(\text{CN})_6^{3-}$ -IRA- 910-MCPE	Injected solution (0.1 mM)	Cu^{2+} -IR- 120-MCPE	$\text{Fe}(\text{CN})_6^{3-}$ -IRA- 910-MCPE
NaNO_3	0.14	0.20	NaCl	0.21	0.23
KNO_3	0.16	0.21	NaBr	0.21	0.24
NH_4NO_3	0.15	0.21	NaHCO_3	0.18	0.17
$\text{Ca}(\text{NO}_3)_2$	0.23	0.32	Na_2SO_4	0.35	0.33
$\text{Mg}(\text{NO}_3)_2$	0.22	0.32	Na_2HPO_4	0.35	0.32
$\text{Al}(\text{NO}_3)_3$	0.37	0.51	NaH_2PO_4	0.39	0.36
			Na_3PO_4	0.35	0.40

Similar variations were observed in the anionic series, the only exception being the response of $\text{Fe}(\text{CN})_6^{3-}$ -IRA-910-MCPE to HCO_3^- (lower than that of Cl^- and Br^- in spite of the same charge), which could be explained by slower mass transport rates of this bigger monovalent anion (in comparison to Cl^- and Br^-).

Such kinetic limitations due to size effects have been previously reported for non-electroactive cations determination at zeolite modified electrodes [28,30]. This can be rationalized by considering that the ion exchange reaction involved in the detection process is (very) far from the equilibrium state, so that it is essentially governed, and therefore limited, by the diffusion of the exchanged and exchanging ions.

In a second time, we have examined the sensors' response to organic acids (and their corresponding anions) likely to be present in typical media where mineral weathering by microorganisms occurs. These species are weak acids, slightly dissociated in aqueous medium. Their amperometric response at $\text{Fe}(\text{CN})_6^{3-}$ -IRA-910-MCPE or Cu^{2+} -IR-120-MCPE would thus depend on the content of free H^+ (to exchange Cu^{2+}) and free anions (to exchange $\text{Fe}(\text{CN})_6^{3-}$). Some informative results have been gathered in Table II. The first observation is a relationship between the intensity of the amperometric response and the pKa (acid dissociation constant) values of the organic acids. For instance, the signal for lactic acid (pKa = 3.08) was larger than that for formic acid (pKa = 3.75) which was also larger than that for acetic acid (pKa = 4.76). This general trend tended to be followed with multi-acids (citric acid (pKa₁ = 3.14; pKa₂ = 4.77; pKa₃ = 6.39); oxalic acid (pKa₁ = 1.23; pKa₂ = 4.19)) except that the larger amount of protons born by these compounds led to even larger amperometric responses. A second feature that can be deduced from Table II is the systematically better sensitivity for the organic acid in comparison to their sodium salt, which is probably due to the higher mobility of protons relative to sodium ions. Again, the sensitivity of $\text{Fe}(\text{CN})_6^{3-}$ -IRA-910-MCPE was superior to that obtained at Cu^{2+} -IR-120-MCPE, so that the former was used throughout hereafter.

Table II: FIA peak currents (μA) sampled for the analysis of various organic acids and their sodium salt (10^{-3} M) using Cu^{2+} -IR-120- or $\text{Fe}(\text{CN})_6^{3-}$ -IRA-910-MCPE at an applied potential of -0.4 V.

Organic acids			Sodium salts		
<u>Injected solution</u> (1 mM)	Cu^{2+} -IR- 120-MCPE	$\text{Fe}(\text{CN})_6^{3-}$ -IRA- 910-MCPE	<u>Injected solution</u> (1 mM)	Cu^{2+} -IR- 120-MCPE	$\text{Fe}(\text{CN})_6^{3-}$ -IRA- 910-MCPE
Oxalic acid	3.3	4.5	Sodium oxalate	2.0	3.3
Citric acid	2.8	4.0	Sodium citrate	2.3	3.1
Lactic acid	2.1	3.0	Sodium lactate	0.8	1.1
Acetic acid	1.2	1.8	Sodium acetate	0.8	1.2
Formic acid	1.9	2.9	Sodium formate	1.1	1.4

Another point, which is of interest with respect to mineral weathering by means of organic acids, is related to the dynamic of organic acid neutralization by a base. An illustrative case is depicted in Fig. 4 for a system based on oxalic acid, calcium hydroxide, and mixtures of these species in various relative concentrations. As expected, the variations of the amperometric response with the concentrations of oxalic acid or calcium hydroxide alone were found to increase in a proportional way, with sensitivity approximately 3 times larger for oxalic acid than for calcium hydroxide. Consistent with results presented in Table II, the progressive neutralization of oxalic acid (*i.e.*, by addition of increasing concentrations of calcium hydroxide, see curve (d) in Fig. 4), leading to the formation of oxalate species, resulted in a decrease of the amperometric response. This decrease is even more pronounced here due to the generation of sparingly soluble calcium oxalate. Finally, when starting from a calcium hydroxide solution, the subsequent addition of oxalic acid in the medium gave rise to a slight increase of amperometric response (see curve (c) in Fig. 4). From these observations, one can thus expect to observe a drop in the amperometric response of the sensor in case of mineral weathering by organic acids because this would lead in their progressive transformation into their anionic counterpart.

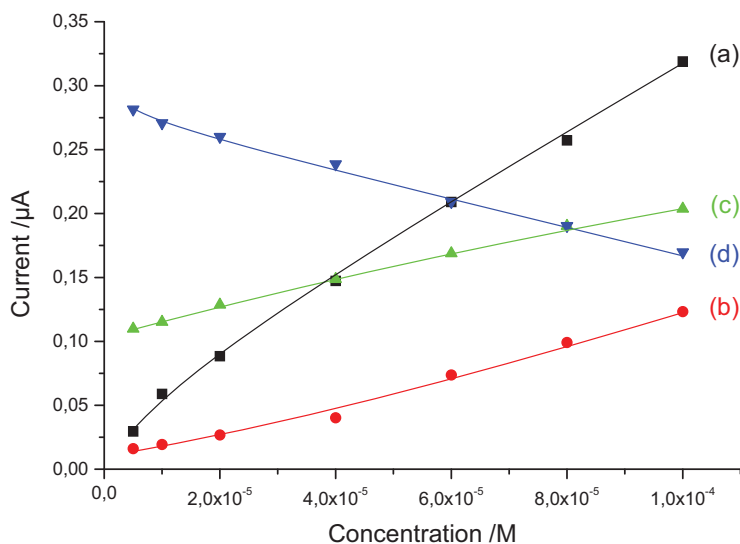


Fig. 4: Variation of the amperometric response of $Fe(CN)_6^{3-}$ -IRA-910-MCPE as a function of (a, c) oxalic acid concentration and (b, d) $Ca(OH)_2$ concentration; (a) oxalic acid alone in pure water; (b) $Ca(OH)_2$ alone in pure water; (c) increasing concentrations of oxalic acid in a medium containing initially 1.0×10^{-4} M $Ca(OH)_2$; (d) increasing concentrations of $Ca(OH)_2$ in a medium containing initially 1.0×10^{-4} M oxalic acid. Other conditions as those in Fig. 2.

Matrix Effects and Application as Bioassay for Mineral Weathering

With respect to the target application, various media of distinct nature and composition are expected to exist. As these media can contain various amounts of ionic species (*i.e.*, different ionic strengths) such ionic matrices would thus contribute to affect the sensor response. Nevertheless, the results presented in Fig. 5 indicate that $\text{Fe}(\text{CN})_6^{3-}$ -IRA-910-MCPE was still sensitive to increasing concentrations of a particular analyte (*i.e.*, $\text{Ca}(\text{NO}_3)_2$ in this case, but the same conclusion can be drawn for other species also tested in this work: NaCl , NaNO_3 , Na_2SO_4 , $\text{Al}(\text{NO}_3)_3$), even in a medium of rather high ionic strength as tap water. However, special care must be taken to establish a calibration curve for each of studied media as the sensitivity was lower and lower when increasing the ionic strength of the matrix, as a result of smaller signal-to-background ratios. The larger background currents observed in higher ionic strength medium are clearly due to the presence of ions that are likely to exchange the redox probes in $\text{Fe}(\text{CN})_6^{3-}$ -IRA-910-MCPE or Cu^{2+} -IR-120-MCPE, contributing thereby to larger background amperometric signals.

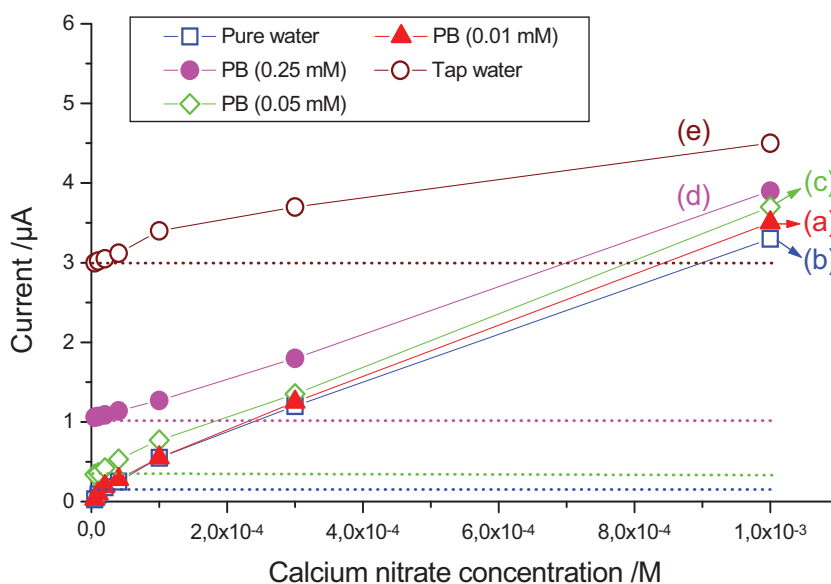


Fig. 5: Variation of the amperometric response of $\text{Fe}(\text{CN})_6^{3-}$ -IRA-910-MCPE as a function of the $\text{Ca}(\text{NO}_3)_2$ concentration in various media; (a) pure water; (b) 10^{-5} M phosphate buffer; (c) 5×10^{-5} M phosphate buffer; (d) 2.5×10^{-4} M phosphate buffer; (e) tap water. Dotted lines indicate the background currents in the absence of added $\text{Ca}(\text{NO}_3)_2$. Other conditions as those in Fig. 4.

We have then evaluated the possibility to use such electrochemical sensor to follow mineral weathering. The first example was chosen as a rather simple one in order to check the validity of the method. It consists in the chemical attack of two zeolite samples exhibiting distinct aluminium/sodium contents (5.6 mmol g^{-1} for NaA and 3.4 mmol g^{-1} for NaY) by citric acid. Indeed, citric acid is known to hydrolyze the aluminium centres in zeolites, liberating thereby sodium, aluminium and citrate ions in solution with concomitant consumption of citric acid. In agreement with the observations made in Fig. 4 and Table II, such transformation would lead to a decrease in the amperometric response of the modified electrodes. This is indeed the case for a solution of citric acid (10^{-4} M) to which increasing zeolite contents were added (see Fig. 6). Moreover, a clear distinction can be made between the two zeolite samples on the basis of their aluminium/sodium contents as the signal variation for zeolite A was larger than for zeolite Y. These results confirm that $\text{Fe}(\text{CN})_6^{3-}$ -IRA-910-MCPE can be indeed used for the qualitative/semi-quantitative evaluation of mineral weathering involving chemical attack by organic acids.

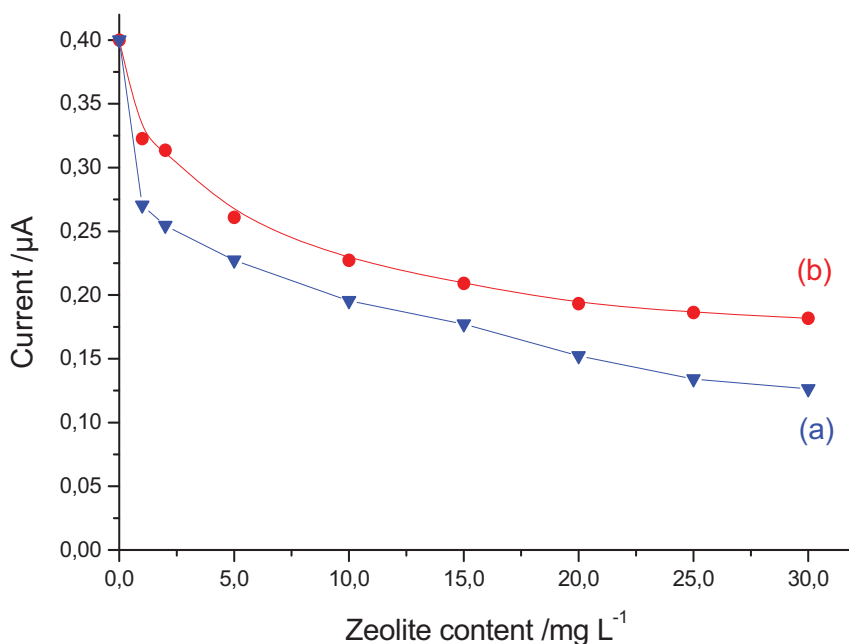


Fig. 6: Variation of the amperometric response of Cu^{2+} -IR-120-MCPE in a 0.1 mM citric acid solution, as a function of the amount of zeolite particles added in suspension; (a) zeolite A; (b) zeolite Y. Other conditions as those in Fig. 4.

Another way of mineral weathering, involving also organic acids, is the biomineralization for which microorganisms likely to generate organic acids are used to solubilise various kinds of minerals. In this study, we have evaluated the biomineralization of 2 olivine samples by mushroom microorganisms. The main ionic element expected to be produced by this process is Mg^{2+} . The analyses were made *in situ* as the crude media (diluted 10-times with pure water) were directly injected in the electrochemical device. On the basis of an appropriate calibration curve established using $Mg(NO_3)_2$, the received amperometric responses corresponded to Mg^{2+} concentrations of respectively 80 ppm (sample A) and 74 ppm (sample B). These values are much lower than those determined by conventional chemical analysis (using inductively-coupled plasma atomic emission spectroscopy, ICP-AES), which revealed total magnesium concentrations of 550 ppm (sample A) and 480 ppm (sample B). But, one has to remind that most magnesium species in such complex media is in a complexed form and, if ICP-AES determines the total amount of magnesium species, the indirect amperometric detector is only sensitive to the free Mg^{2+} ions. The interesting feature here is not the observed absolute values, but the signal ratio obtained between the two samples ($80/74 = 1.08$) which correlates quite well with the total magnesium concentration ratio determined by ICP-AES ($550/480 = 1.14$). One can thus consider that the amperometric detection of non-electroactive species can be applied as an electrochemical bioassay, yet qualitative, for monitoring of the biological weathering of minerals.

Conclusions

Carbon paste electrodes modified with organic polymers doped with cationic or anionic redox probes (Cu^{2+} or $Fe(CN)_6^{3-}$) can be used as sensitive electrochemical sensors for the indirect amperometric detection of non-electroactive ions and weakly dissociated organic acids. When performed in FIA mode and in the absence of added supporting electrolyte, the current response is due to the sum of a capacitive component due to conductivity change when the analyte passes the electrode surface and a faradic part arising from the reduction of redox probes liberated by ion exchange with the analyte. This detection scheme can be basically applied to monitor any process involving significant variation in the ionic strength of the medium. We have pointed out here that the method constitutes a promising qualitative or semi-quantitative electrochemical test for mineral weathering.

Acknowledgements

Financial support from the "ACI Ecologie Quantitative" (project № 1317A, "Quantification de l'altération biologique des minéraux du sol") is gratefully acknowledged. The authors would also like to thank Mr. M. El Akroute for help in the experiments.

References

1. R.L. Solsky: *Anal. Chem.* **62** (1990) 21R.
2. E. Pretsch: *Trends Anal. Chem.* **26** (2007) 46.
3. J. Bobacka, A. Ivaska, A. Lewenstam: *Chem. Rev.* **108** (2008) 329.
4. E. Bakker, K. Chumbimuni-Torres: *J. Braz. Chem. Soc.* **19** (2008) 621.
5. M. Rezapour, M.R. Ganjali, P. Perviz, F. Faridbod; in: *Electrochemical Sensors* (M.R. Ganjali, P. Norouzi, F. Faridbod, Eds.), pp. 1-35. Research Signpost, Trivandrum, Kerala, India, 2010.
6. Y. Ikariyama, W.R. Heineman: *Anal. Chem.* **58** (1986) 1803.
7. J. Ye, R.P. Baldwin: *Anal. Chem.* **60** (1988) 1979.
8. K.N. Thomsen, R.P. Baldwin: *Anal. Chem.* **61** (1989) 2594.
9. K.N. Thomsen, R.P. Baldwin: *Electroanalysis* **2** (1990) 263.
10. E. Wang, A. Liu: *Anal. Chim. Acta* **252** (1991) 53.
11. M.D. Baker, C. Senaratne: *Anal. Chem.* **64** (1992) 697.
12. P. Ward, M. R. Smyth: *Talanta* **40** (1993) 1131.
13. R. C. Martinez, F.B. Dominguez, F.M. Gonzalez, J.H. Mendez, R.C. Orellana: *Anal. Chim. Acta* **279** (1993) 299.
14. O. Sadik, G.G. Wallace: *Electroanalysis* **5** (1993) 555.
15. O. Sadik, G.G. Wallace: *Electroanalysis* **6** (1994) 860.
16. A. Walcarius, L. Lamberts, E.G. Derouane: *Electroanalysis* **7** (1995) 120.
17. R. Liu, B. Sun, D. Liu, A. Sun: *Talanta* **43** (1996) 1049.
18. R. John, D.M. Ongarato, G.G. Wallace: *Electroanalysis* **8** (1996) 623.
19. J. N. Barisci, G.G. Wallace, A. Clarke: *Electroanalysis* **9** (1997) 461.
20. P. Akhtar, C.O. Too, G.G. Wallace: *Anal. Chim. Acta* **339** (1997) 201.
21. G. Tavcar, K. Kalcher, B. Ogorevc: *Analyst* **122** (1997) 371.
22. H.J. Lee, P.D. Beattie, B.J. Seddon, M.D. Osborne, H.H. Girault: *J. Electroanal. Chem.* **440** (1997) 73.

23. H.J. Lee, H. H. Girault: *Anal. Chem.* **70** (1998) 4280.
24. H.J. Lee, C. Beriet, H. H. Girault: *Anal. Sci.* **14** (1998) 71.
25. H.J. Lee, C. Beriet, H. H. Girault: *J. Electroanal. Chem.* **453** (1998) 211.
26. S. Sawada, H. Torii, T. Osakai, T. Kimoto: *Anal. Chem.* **70** (1998) 4286.
27. A. Walcarius, L. Lamberts: *Anal. Lett.* **31** (1998) 585.
28. A. Walcarius: *Anal. Chim. Acta* **388** (1999) 79.
29. A. Walcarius, V. Vromman, J. Bessière: *Sensors Actuators B* **56** (1999) 136.
30. A. Walcarius, P. Mariaulle, C. Louis, L. Lamberts: *Electroanalysis* **11** (1999) 393.
31. C. Fu, L. Wang, Y. Fang: *Anal. Chim. Acta* **391** (1999) 29.
32. E. Staes, L. J. Nagels: *Talanta* **52** (2000) 277.
33. Q. Xu, C. Xu, Y. Wang, W. Zhang, L. Jin, K. Tanaka, H. Haraguchi, A. Itoh: *Analyst* **125** (2000) 1453.
34. H.J. Lee, C.M. Pereira, A.F. Silva, H.H. Girault, *Anal. Chem.* **72** (2000) 5562.
35. A. Ceresa, E. Pretsch, E. Bakker: *Anal. Chem.* **72** (2000) 2050.
36. A. Walcarius, P. Mariaulle, L. Lamberts: *J. Solid State Electrochem.* **7** (2003) 671.
37. J.-J. Xu, N. Bao, X.-H. Xia, Y. Peng, H.-Y. Chen: *Anal. Chem.* **76** (2004) 6902.
38. J.-J. Xu, Y. Peng, N. Bao, X.-H. Xia, H.-Y. Chen: *Electrophoresis* **26** (2005) 3615.
39. H. Ge, G.G. Wallace: *React. Polym.* **18** (1992) 133.
40. A. Walcarius: *Electroanalysis* **8** (1996) 971.
41. A. Walcarius: *Anal. Chim. Acta* **384** (1999) 1.
42. A. Walcarius, L. Lamberts, E. G. Derouane: *Electrochim. Acta* **38** (1993) 2267.
43. P. Mariaulle, F. Sinapi, L. Lamberts, A. Walcarius: *Electrochim. Acta* **46** (2001) 3543.
44. W.W. Barker, S.A. Welch, J.F. Banfield: *Rev. Mineral.* **35** (1997) 391.
45. J. Berthelin, C. Leyval, C. Mustin: *Mineral. Soc. Ser.* **9** (2000) 7.
46. J. Berthelin, C. Leyval C.: *Plant Soil* **68** (1982) 369.
47. C. Balland., A. Poszwa, C. Leyval, C. Mustin: *Geochim. Cosmochim. Acta* **74** (2010) 5478.
48. E. Valsami Jones, S. McEldowney: *Mineral. Soc. Ser.* **9** (2000) 27.
49. P. Hinsinger, C. Plassard, B. Jaillard, Benoit: *J. Geochem. Explor.* **88** (2006) 210.
48. H. Lambers, C. Mougél, B. Jaillard, P. Hinsinger: *Plant Soil* **321** (2009) 83.
50. S. Uroz, C. Calvaruso, M.P. Turpault, P. Frey Klett: *Trends Microbiol.* **17** (2009) 378.

